Biomedical Signal Processing and Control 11 (2014) 97–106

Contents lists available at ScienceDirect

Biomedical Signal Processing and Control

journal homepage: www.elsevier.com/locate/bspc

2D ECG differences in frontal vs preferential planes inpatients referred for percutaneous transluminal coronary angioplasty☆

María Paula Bonomini[a,*], Sebastián Javier Corizzo[a], Pablo Laguna[b,c], Pedro David Arini[a,d]

[a] Instituto de Ingeniería Biomédica, Facultad de Ingeniería, Universidad de Buenos Aires, Argentina
[b] Grupo de Tecnología de Comunicaciones, Instituto de Investigaciones en Ingeniería de Aragón (I3A), Zaragoza, Spain
[c] Centro de Investigación Biomédica en Red (CIBER-BBN), Spain
[d] Instituto Argentino de Matemática, 'Alberto P. Calderón' CONICET, Buenos Aires, Argentina

ARTICLE INFO

Article history:
Received 1 October 2013
Received in revised form
20 December 2013
Accepted 20 January 2014

Keywords:
Frontal plane
PCA-transformed ECG
Electrical cardiac axis
Cardiac vectors
Ventricular gradient

ABSTRACT

This work proposes a comparative study of a pair of electrocardiographic 2D representations: the frontal plane (FP) and a preferential plane (PP) obtained from ECG data. During depolarization and repolarization, main electrical vectors were analyzed and compared between healthy subjects and patients referred for percutaneous transluminal coronary angioplasty (PTCA). Recordings were obtained at rest. Many patients from the latter group presented normal ECGs, thus, the hypothesis to prove was that electrical axis in any of the studied planes would effectively discriminate silent ischemia records from healthy ones. The FP was constructed with I and aVF leads, while the PP used the two first eigenvectors of the spatial correlation matrix of the ECG. Although the depolarization and repolarization vectors from both groups resulted normal, those from the silent ischemia group appeared strongly biased to the left, closer to the limit of the normality range. This slight change originated a significant separation between health and disease in the FP. Here, most of the parameters resulted highly informative, even those related to the depolarization phase. The cardiac vector, integrating both depolarization and repolarization information, presented the highest performance (AUC = 0.89). Parameters in the PP, however, did not produce an acceptable discrimination, except for the amplitude of the T-wave (AUC = 0.79). Additionally, the repolarization orientation in the FP was the only marker that simultaneously discriminated three different groups of patients according to their occlusion sites ($p < 0.0001$). In conclusion: the FP offered a 2D representation general enough to enable the separation of silent ischemia versus health populations while the PP did not, due mainly to its individually optimized nature, failing to provide a unique referencial frame for all the subjects.

1. Introduction

Myocardial ischemia occurs due to an imbalance between myocardial oxygen supply and demand. This phenomenon is frequently associated with coronary atherosclerosis, which hinders the normal coronary artery blood flow. An insufficient myocardial cell irrigation is accompanied by a succession of electrophysiological modifications that affect cardiac ventricular repolarization [1,2]. These repolarization changes are reflected in the electrocardiogram (ECG) as ST-segment [3] and T-wave morphology modifications [4]. Others reported depolarization changes accompanying ischemia as well. Particular examples are: decrease of upward and downward slopes of the QRS-complex during coronary artery occlusion [5], changes in QRS amplitudes [6,7], changes in QRS-complexes duration [8], angular modifications [9] and even changes in vectocardiographic QRS-loop parameters [10].

In general, the duration and morphology changes of the depolarization or the repolarization phenomenon during an ischemic episode are analyzed individually [11,12]. In addition to the individual analysis, we also looked for depolarization and repolarization phases relationships using certain concepts of ventricular gradient with the aim to improve ischemic diagnosis.

The idea of the ventricular gradient, calculated as the difference in the global orientation and extent of the QRS-complex and of the T-wave, was proposed by Wilson et al. as early as the 1930s [13]. The most important use of it is to identify primary and secondary T-wave abnormalities in the ECG [14]. A secondary T-wave puts into evidence ventricular conduction abnormalities. A primary T-wave calls attention to several possible disorders such as tachycardia or bradycardia, hypokalemia or hyperkalemia local ischemia and even necrosis [15].

☆ This work was supported by the Consejo Nacional de Investigaciones Científicas y Técnicas, under Project PIP-538 CONICET, Argentina.
* Corresponding author.
E-mail address: paulabonomini@gmail.com (M.P. Bonomini).

1746-8094/$ – see front matter © 2014 Elsevier Ltd. All rights reserved.
http://dx.doi.org/10.1016/j.bspc.2014.01.006

Expanding the old ventricular gradient concept, the angle of the 3D between QRS-complex and T-wave loops in the Principal Component Analysis (PCA) space was proposed [16]. This 3D descriptor, so-called Total Cosine R-to-T (T_{crt}), proved to be a good cardiac risk predictor in different groups of patients, including survivors of acute myocardial infarction and patients with known ischemic heart diseases [17], as well as in the general population [18,19].

Myocardial ischemia is usually diagnosed by means of a stress test. In asymptomatic patients, which is the case for silent ischemia, the decision to perform a stress test is based upon estimation of the absolute risk of any cardiac event during the following 10 years, together with the familiar history of coronary heart disease risk [20]. A stress test is a rather complex test, requiring many resources and time from the healthcare system. The modalities used to document any abnormal stress response include the electrocardiogram, echocardiography, radionuclide imaging with either single photon emission computed tomography or positron emission tomography, and magnetic resonance imaging.

Another spatiotemporal technique called cardiogoniometry (CGM) has been proposed for myocardial ischemia detection, as an alternative to ECG analysis [21]. CGM is an orthogonal representation of the cardiac activity onto two orthogonal planes: the frontal plane and the oblique sagittal plane. The improvement introduced with respect to vectorcardiography is that planes are oriented in rough approximation to the anatomy of the heart, rather than the body. Recently, Huebner and collaborators have classified ischemic patients and healthy subjects using cardiogoniometric parameters [22].

In order to find a fast and inexpensive first diagnosis of myocardial ischemia that allows to reduce the amount of stress tests indications, we focused on the analysis of cardiac vectors in two bidimensional representations derived from the ECG, such as the frontal plane (FP), defined by the Einthoven's triangle, and a preferential plane (PP), obtained from applying PCA methods to the ECG data. The hypothesis behind this study relies on the fact that the FP is an individual-independent frame. That is, orientation of the main vectors are independent on individuals, while the PCA transformed space can be seen as a frontal plane undergoing an individual-dependent rotation which captures most of the ECG energy for each subject. According to this, the PP would act as an individually optimized frontal plane.

The principal objective of the study aimed at comparing the ability of these two representations of the ECG (the frontal plane and the preferential plane) to separate ischemic patients from healthy subjects. To accomplish the objective, we studied two parameters, angle and modulus of the depolarization and repolarization dominant vectors in the above mentioned planes.

2. Materials and methods

2.1. Population

The study population was composed of two groups, one consisting of ECG records from 52 healthy subjects obtained from the Physikalish Technisque Bundesanstalt (PTB) database (39 men, age 42 ± 14 yrs, and 13 women, age 48 ± 19 yrs), provided by the National Institute of Metrology of Germany, conceived with educational, algorithm benchmarking and research purposes [23,24]. ECG records were obtained with a non-commercial device consisting of 16 input channels (15 for ECG: I, II, III, aVR, aVL, aVF, V_1–V_6, Vx, Vy, Vz and 1 for respiration), each of them acquired at 1000 Hz. Even though the PTB database also contained pathologic ECG records, we limited its usage to control subjects. The second group consisted of resting ECG records from 83 patients (52 men, age 62 ± 14, 31 females, age 65 ± 11) at the Charleston Area Medical Center in West Virginia before undergoing elective prolonged balloon occlusion during percutaneous transluminal coronary angioplasty (PTCA), in one of the major coronary arteries (STAFF-III study). This study was approved by the Investigational Review Board. Informed consent was obtained from each subject [3,25]. Eight leads (V_1–V_6, I, II) were recorded using equipment by Siemens-Elena AB (Solna, Sweden) and digitized at sampling rate of 1000 Hz and amplitude resolution of 0.6 μV. Leads III, aVR, aVL and aVF were derived from leads I and II. Two control recordings were acquired continuously for five minutes in supine position prior to the PTCA procedure in clinical stable conditions, within a time interval of a maximum of 1 hour. The electrodes were maintained on the patients between both recordings, or changed and their positions marked, to enable accurate comparisons of the ECG variables.

2.2. ECG preprocessing

Signal preprocessing was applied on the 12 standard or 8 linearly independent leads of the ECG data (PTB and STAFF-III databases respectively). QRS detection and selection of normal beats were implemented according to the method in [26], cubic spline interpolation was used for baseline wander attenuation. Rejection of noisy beats was implemented when differences in mean isoelectric level with respect to adjacent beats were larger than 300 μV. The QRS-complexes and T-waves were located and delineated using the wavelet transform method, as in [27].

2.3. Frontal plane indexes

The FP was defined by the standard and augmented limb leads (I, II, III, aVR, aVL and aVF). More specifically, the frontal representation consisted of constructing the QRS and T-wave loops defined by lead I (L_{I}) and lead aVF (L_{aVF}). First, segmentation of the QRS-complex and T-wave was accomplished for each ith beat using a single lead criteria where the onset of the QRS-complex and the T-wave were the earliest reliable QRS-complex and T-wave onset at L_{I} or L_{aVF} and the offsets, the latest reliable QRS-complex and T-wave offset in the same leads. On these segmented waves, the QRS-loop and the T-loop for each ith beat were constructed and both cardiac vectors computed at the loop samples $n \in W_i^{\mathrm{QRS}}$ and $n \in W_i^{\mathrm{T}}$, representing the QRS-complex and T-wave windows respectively. The sample $n_{\max}^{\mathrm{QRS}}(i)$ and $n_{\max}^{\mathrm{T}}(i)$ at which the respective QRS and T cardiac vectors resulted maximum were computed. Then, the modulus and angle of the QRS-complex main cardiac vector for the ith beat, $R_f^{\alpha}(i)$ and $R_f^{m}(i)$ respectively, were defined as:

$$R_f^{\alpha}(i) = \operatorname{atan}\left(\frac{L_{\mathrm{aVF}}(n_{\max}^{\mathrm{QRS}}(i))}{L_{\mathrm{I}}(n_{\max}^{\mathrm{QRS}}(i))}\right) \tag{1}$$

$$R_f^{m}(i) = \sqrt{L_{\mathrm{I}}(n_{\max}^{\mathrm{QRS}}(i))^2 + L_{\mathrm{aVF}}(n_{\max}^{\mathrm{QRS}}(i))^2} \tag{2}$$

where

$$n_{\max}^{\mathrm{QRS}}(i) = \underset{n}{\operatorname{argmax}}\left[\sqrt{L_{\mathrm{I}}(n)^2 + L_{\mathrm{aVF}}(n)^2}\right] \tag{3}$$

where $n \in W_i^{\mathrm{QRS}}$

Analogously, the modulus and angle of the T-wave maximum cardiac vector for the ith beat, $T_f^{\alpha}(i)$ and $T_f^{m}(i)$ respectively, were defined as:

$$T_f^{\alpha}(i) = \operatorname{atan}\left(\frac{L_{\mathrm{aVF}}(n_{\max}^{\mathrm{T}}(i))}{L_{\mathrm{I}}(n_{\max}^{\mathrm{T}}(i))}\right) \tag{4}$$

$$T_f^{m}(i) = \sqrt{L_{\mathrm{I}}(n_{\max}^{\mathrm{T}}(i))^2 + L_{\mathrm{aVF}}(n_{\max}^{\mathrm{T}}(i))^2} \tag{5}$$

where

$$n^{\mathrm{T}}_{\max}(i) = \underset{n}{\mathrm{argmax}} \left[\sqrt{L_{\mathrm{I}}(n)^2 + L_{\mathrm{aVF}}(n)^2} \right] \quad (6)$$

where $n \in W_i^{\mathrm{T}}$

The depolarization and repolarization equivalent vector components for the ith beat $RT^{\alpha}_{\mathrm{F}}(i)$ and $RT^{m}_{\mathrm{F}}(i)$ were computed as the following vectorial sum:

$$RT^{\alpha}_{\mathrm{F}}(i) = \mathrm{atan}\left(\frac{R_y(i) + T_y(i)}{R_x(i) + T_x(i)} \right) \quad (7)$$

$$RT^{m}_{\mathrm{F}}(i) = \sqrt{(R_x(i) + T_x(i))^2 + (R_y(i) + T_y(i))^2} \quad (8)$$

where $R_x(i)$ and $R_y(i)$ are the cartesian components of $[R^{\alpha}_f(i), R^{m}_f(i)]$ and $T_x(i)$ and $T_y(i)$ are the cartesian components of $[T^{\alpha}_f(i), T^{m}_f(i)]$. We will refer to this vector as the cardiac vector.

2.4. Preferential plane indexes

In [16] there is a detailed explanation about the ECG decomposition onto the PCA space. Briefly, the *N times M* ECG matrix **X** undergoes the singular value decomposition (SVD). Here, N is conformed by the 8 independent ECG leads (I, II, V_1–V_6) and M accounts for the samples of the recordings. Thus, the ECG data can be expressed as $\mathbf{X} = \mathbf{U}\ \Sigma\mathbf{V}^T$, where **U** is an 8×8 matrix whose columns are the left singular vectors, **V** is an $M \times M$ matrix whose columns are the right singular vectors and Σ is an $8 \times \mathrm{M}$ non-negative diagonal matrix containing the singular values $\sigma_1, \ldots, \sigma_N$. This decomposition rotates the ECG matrix **X** in an 8-dimensional space represented by 8 singular values contained in the Σ matrix and 8 singular vectors contained in the columns of **U**.

After PCA, the windows W_i^{R} and W_i^{T} corresponding to the QRS-complex and T-wave at each beat were defined by delineating a norm signal defined as $E_{2D}(n) = \sqrt{\mathrm{s12(n)} + \mathrm{s22(n)}}$, where $s_1(n)$ and $s_2(n)$ are the projections of the ECG data matrix **X**, onto the two first eigenvectors u_1 and u_2 associated to the SVD in the equation $\mathbf{S} = \mathbf{U}^T\mathbf{X}$. Delineation was modified from [16] for the two-dimensional case.

QRS- and T-loops were constructed for each ith beat. A cardiac vector was computed at the loop samples $n \in W_i^{\mathrm{R}}$ and $n \in W_i^{\mathrm{T}}$, selecting the sample $n^{\mathrm{R}}_m(i)$ and $n^{\mathrm{T}}_m(i)$ at which the depolarization and repolarization cardiac vector was maximum. The modulus and angle of the main depolarization vector for the ith beat, $R^{\alpha}_p(i)$ and $R^{m}_p(i)$ respectively, as well as the modulus and angle of the T-wave maximum cardiac vector for the ith beat, $T^{\alpha}_p(i)$ and $T^{m}_p(i)$ and the depolarization and repolarization equivalent vector components for the ith beat $RT^{\alpha}_{\mathrm{P}}(i)$ and $RT^{m}_{\mathrm{P}}(i)$ were defined as in (1)-(8).

2.5. Loops alignment

In order to compensate for changes induced by respiratory movements, an alignment of all QRS-loops and T-loops was carried out [28]. To do this, rotation (R_{al}) and translation (T_{al}) matrices were calculated to align beat-to-beat loops against a template loop. The latter was computed by averaging the temporally aligned QRS-complex or T-wave in the respective leads (Lead I and Lead aVF for the FP or $s_1(n)$ and $s_2(n)$ for the PP) at the first minute of each record using the standard methodology [29]. Such R_{al} and T_{al} matrices were computed from an adapted version of the algorithm [30], as follows:

1. Coordinates $L_{\mathrm{I}}(i)$ and $L_{\mathrm{aVF}}(i)$ (or $s_1(i)$ and $s_2(i)$) of the pattern loop and the individual loops were grouped into p_i and q_i sets respectively, with $i = 1, \ldots, N$, N standing for the total number of samples of the segmented signal to align.
2. Both sets p_i and q_i were arranged in two $3 \times N$ matrices, designed as **P** and **Q**, respectively. Then, the covariance matrix **H** was defined as $\mathbf{QP}^T$.
3. The matrices **U**, Σ and **V** were obtained by applying SVD to the **H** matrix: $\mathbf{H} = \mathbf{U}\Sigma\mathbf{V}^T$. Therefore, $R_{al} = \mathbf{VU}^T$.
4. The translation matrix was calculated as the difference between the coordinates of the QRS-loop centroid (p_c) and the centroid of the individual QRS-loop (q_c), that is $T_{al} = p_c - R_{al} \times q_c$.

2.6. Statistical analyses

All data were expressed as mean ± SD. The D'Agostino–Pearson normality test was applied to quantify the discrepancy between the distribution of the indexes and an ideal Gaussian distribution. In order to determine the statistical power of each marker to discriminate health from ischemia, a non-parametric two-tailed Mann–Whitney test was applied between healthy and ischemic patients. When p-value was <0.05, differences were considered statistically significant.

2.7. Classification and ROC analysis

We calculated the Receiver Operating Characteristic (ROC) curves for every parameter and plotted the sensitivity against the 1-specificity values for the different possible cut-off points. Thereafter, the optimal cut-off point in the ROC curve was computed as the point nearest the top left-hand corner. This selection maximizes the sensitivity and specificity sum, when it is assumed that the 'cost' of a false negative result is the same as that of a false positive result [31].

3. Results

The total population was studied here, without making any distinction on the dilation site at the group of patients referred for PTCA. For all the studied groups along this work, indexes did not follow a Gaussian distribution, not even after applying logarithms.

As an example, Fig. 1 shows the loops constructed under the frontal and the preferential planes for the depolarization (dotted line) and the repolarization phase (solid line) in two different patients, one belonging to the control or healthy group and the other belonging to the PTCA patients. Arrows depict main electrical vectors for each phase. For clarity sake, depolarization and repolarization loops are only labeled in Fig. 1b. Since loops keep their size proportion nearly constant, QRS-complex and T-wave loop recognition is evident for the remaining panels.

It is worth noticing the wide average age difference between groups. In order to search for an eventual correlation between the parameters involved in this study and age for both populations, the Pearson's correlation coefficient r between age and every parameter was computed. Since r-values were close to 0 and p-values were greater than 0.05, it can be proved that there is no significant correlation between the parameters measured over the depolarization/repolarization vectors and the patients age.

3.1. Descriptive statistics

3.1.1. Frontal plane

Fig. 2a and c displays the mean ± SD depolarization and repolarization angles (R^{α}_f and T^{α}_f), while Fig. 2b and d depicts the mean ± SD moduli (R^{m}_f and T^{m}_f) of control subjects versus ischemic patients on the upper four panels.

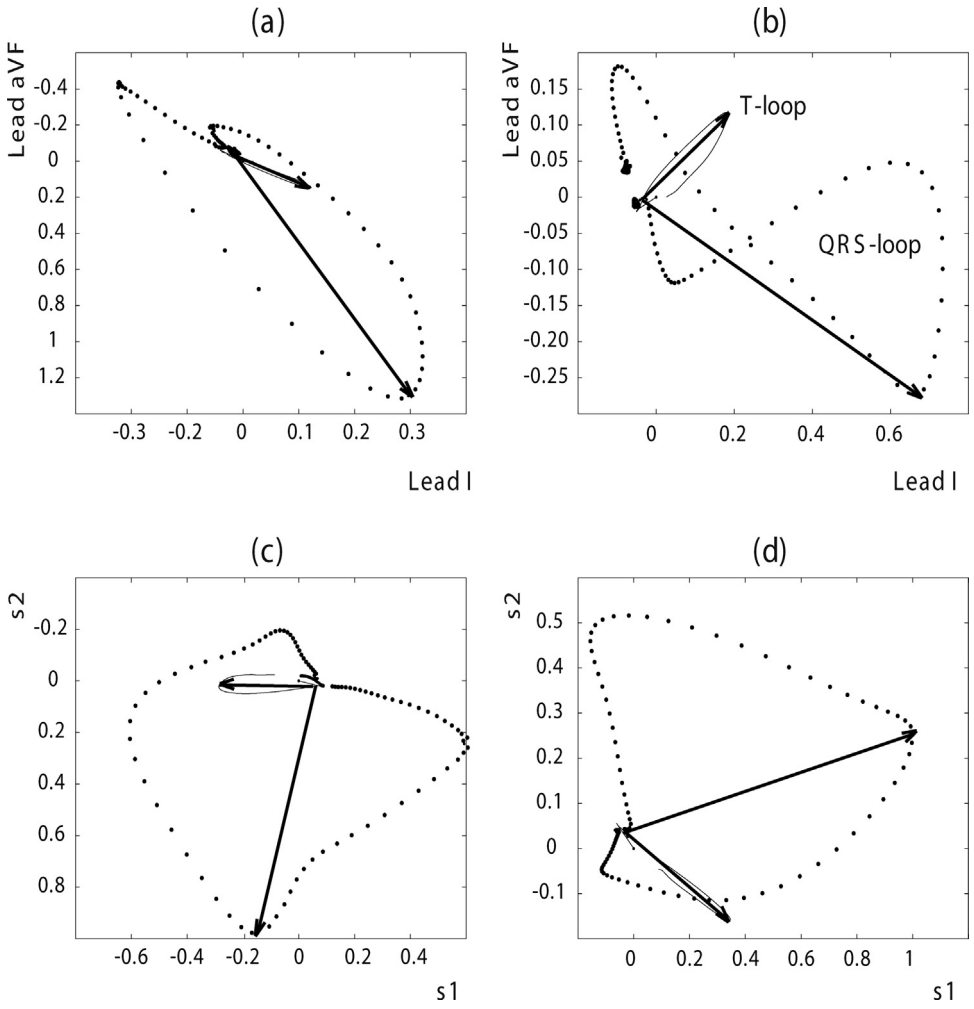

Fig. 1. Representative examples of cardiac activity in terms of depolarization (dotted line) and repolarization (solid line) loops for each cardiac phase (arrows). Loops were constructed with Leads I and aVF in the frontal plane and *s*1 and *s*2 pseudo-leads in the preferential plane. Each point in the loop represents a voltage for each of the two leads at a particular time bin. Depolarization and repolarization loops are only labeled in (b). Since they keep the same proportions in all cases. (a) Healthy subject in the FP, (b) PTCA patient in the FP, (c) healthy subject in the PP, (d) PTCA patient in the PP.

Depolarization and repolarization angles were positive in both groups. Moreover, the average angles for the PTCA group in the two cardiac phases were significantly lower than those of the healthy subjects (depolarization: healthy subjects $57.88 \pm 29.56^\circ$, PTCA patients $26.90 \pm 26.45^\circ$, $p < 0.0001$, repolarization: healthy subjects $50.79 \pm 9.54^\circ$, PTCA patients $23.21 \pm 58.79^\circ$, $p < 0.001$). T-wave angle variability in the health group was lower than those of the ischemic group, while QRS-complex angle variability kept constant among groups. Note that even though angles presented normal values for both groups, the disease group showed values biased to the left, in the limit of the normality range [32,33].

Opposite to angles, amplitudes resulted much more variable in the case of health. In silent ischemia, amplitudes suffered significantly in both phases with respect to the control group (depolarization: healthy subjects 1.31 ± 0.61 mV, ischemic patients 0.80 ± 0.28 mV, $p < 0.0001$, repolarization: healthy subjects 0.28 ± 0.13 mV, ischemic patients 0.12 ± 0.05 mV, $p < 0.05$). Furthermore, amplitudes presented much less variability in disease.

Consistently, the angle and amplitude of the cardiac vector, obtained by vectorially summing the QRS-complex and T-wave dominant vectors calculated as in (7) and (8), significantly discriminated health from ischemia (angle: healthy subjects $-57.67 \pm 24.98^\circ$, PTCA patients $-26.77 \pm 27.06^\circ$, $p < 0.0001$, modulus: healthy subjects 1.62 ± 0.80 mV, PTCA patients 0.87 ± 0.29 mV, $p < 0.0001$) (see Fig. 3c). Note the increase of angle variability from health to disease in the repolarization phase, while the depolarization angle variability in the same plane decreased from health to disease. On the other hand, amplitude variability decreased from health to disease in both phases (see Fig. 3a). Another measure taken into account was the angle between the depolarization and repolarization phases, which in this case decreased from $-7.08 \pm 30.18^\circ$ to $-4.51 \pm 70.49^\circ$, although failed to give any statistical significance. Notice that this last measure recalls the traditional concept of the ventricular gradient, in its bidimensional form.

3.1.2. Preferential plane

Fig. 2e and g displays the mean ± SD depolarization and repolarization angles (R_t^α, T_t^α) and Fig. 2f and h displays the mean ± SD moduli (R_t^m, T_t^m) of control subjects versus ischemic patients on the lower four panels.

Average angles in either cardiac phase did not significantly differentiated ischemia from health (depolarization: healthy subjects $-10.85 \pm 54.15^\circ$, ischemic patients $-10.64 \pm 61.67^\circ$, $p = 0.79$, repolarization: healthy subjects $-59.69 \pm 78.06^\circ$, ischemic patients $-32.12 \pm 95.02^\circ$, $p = 0.10$). Unlike the FP, angle variability here remained constant for both groups (see Fig. 3b).

Analogously to the frontal plane, amplitudes did discriminate both groups either in the depolarization as the repolarization

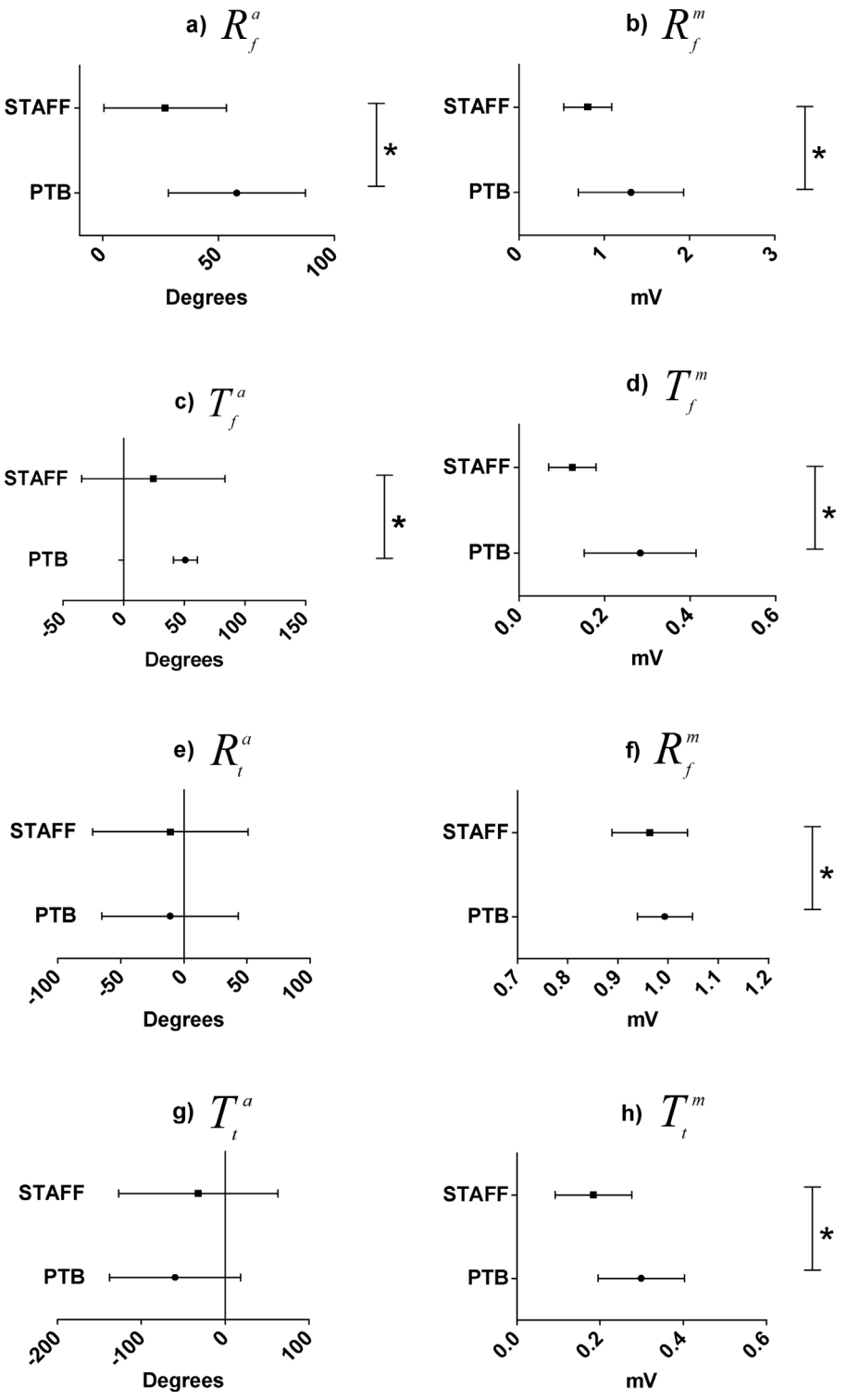

Fig. 2. Descriptive statistics for every parameter analyzed in both planes for the two groups. (a) Mean ± SD angle of the depolarization vector in the FP (R_f^α), (b) mean ± SD modulus of the depolarization vector in the FP (R_f^m), (c) mean ± SD angle of the repolarization vector in the FP (T_f^α), (d) mean ± SD modulus of the repolarization vector in the FP (T_f^m), (e) mean ± SD angle of the depolarization vector in the PP (R_t^α), (f) modulus of the depolarization vector in the PP (R_t^m), (g) mean ± SD angle of the repolarization vector in the PP (T_t^α), (h) mean ± SD modulus of the repolarization vector in the PP (T_t^m), $^*p < 0.0001$, $^{**}p < 0.005$.

phase. (depolarization: healthy subjects 0.99 ± 0.05 mV, PTCA patients 0.96 ± 0.07 mV, $p < 0.05$, repolarization: healthy subjects 0.29 ± 0.10 mV, PTCA patients 0.18 ± 0.09 mV, $p < 0.001$). Amplitude variability here also kept constant for health or disease (see Fig. 3b).

Finally, angle of the equivalent cardiac vector, calculated as the resultant vector between the QRS-complex and T-wave dominant vectors, did not significantly separate health from the silent ischemic group (angle: healthy subjects −19.42 ± 57.30°, PTCA patients −14.81 ± 62.65°, $p = 0.72$) but did the modulus (healthy subjects 1.12 ± 0.19, PTCA patients 1.02 ± 0.14, $p < 0.01$). Notice here, how the equivalent cardiac vector picked up the large variability behavior from the isolated phases. Additionally, angle

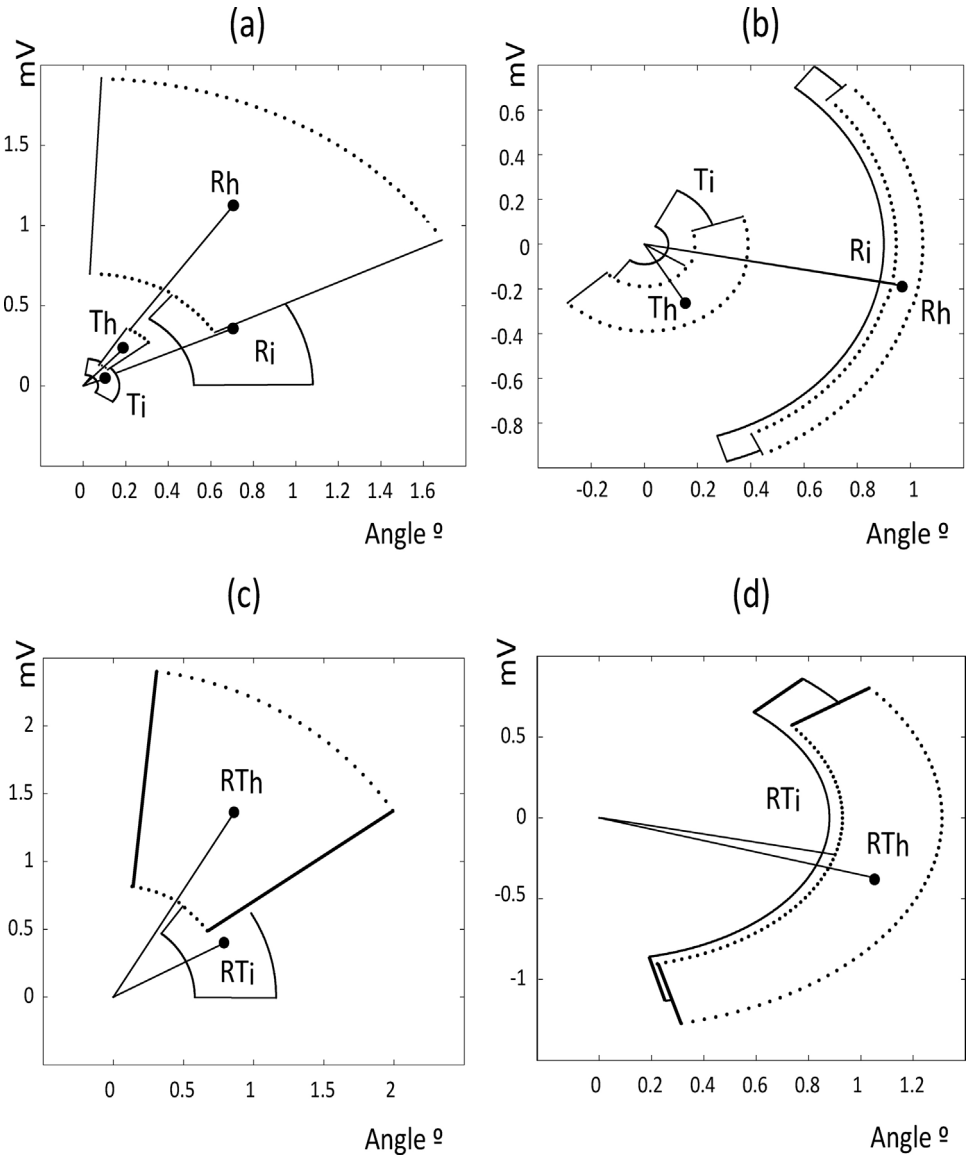

Fig. 3. Main average depolarization, repolarization and cardiac vectors for the frontal and preferential planes. Boxes account for the standard deviations in amplitude and angles of the mean modulus (dot) and the mean angle (line) comprising each vector. (a) FP depolarization and repolarization vectors in health, R_f^h and T_f^h (dotted box), FP depolarization and repolarization vectors in ischemia, R_f^i and T_f^i (solid box), (b) PP depolarization and repolarization vectors in health, R_t^h and T_t^h (dotted box), PP depolarization and repolarization vectors in ischemia, R_t^i and T_t^i (solid box), (c) FP equivalent cardiac vector in health, RT_f^h (dotted box) and FP equivalent cardiac vector in ischemia, RT_f^i (solid box), (d) PP equivalent cardiac vector in health, RT_t^h (dotted box) and PP equivalent cardiac vector in ischemia RT_t^i (solid box).

and amplitude variability kept mostly constant for health and disease (see Fig. 3d). Lastly, the angle between the depolarization and repolarization phases diminished from $52.50 \pm 80.68^\circ$ to $22.58 \pm 116.63^\circ$, but no statistical significance was found.

3.2. ROC analysis

In Fig. 4, the ROC curves for every parameter and their area under the curve (AUC) values are shown. In the FP, most of the parameters resulted highly informative, even those related to the depolarization phase (see Fig. 4a and b), with the exception of the repolarization direction, which showed a moderate AUC value (see Fig. 4c). Although the cardiac vector in this plane, which integrates both depolarization and repolarization information, presented good ROC curves, it failed to dramatically improve the performance achieved by the depolarization or repolarization phases alone (see Fig. 4e and f). The modulus of the repolarization main vectors presented good AUC values on both planes (see Fig. 4d and j). Parameters in the PP, however, provided poor performance. Angles either for the depolarization and the repolarization phases presented AUC values near 0.5, suggesting that performance of classification was close to a "by-chance" process. In this plane, only the amplitude parameters seemed to reach an acceptable balance between sensitivity and specificity (see Fig. 4k and l). Moreover, the cardiac vector in this plane did not add valuable information to that offered by the separated depolarization and repolarization phases.

3.3. Ischemia localization

In order to test whether any parameter from any proposed plane was able to differentiate the coronary artery sites to perform the PTCA, we split up the STAFF-III database according to dilation sites. The location of the 83 dilations were: left anterior descendent coronary artery (LAD) in 25 patients, left circumflex coronary artery

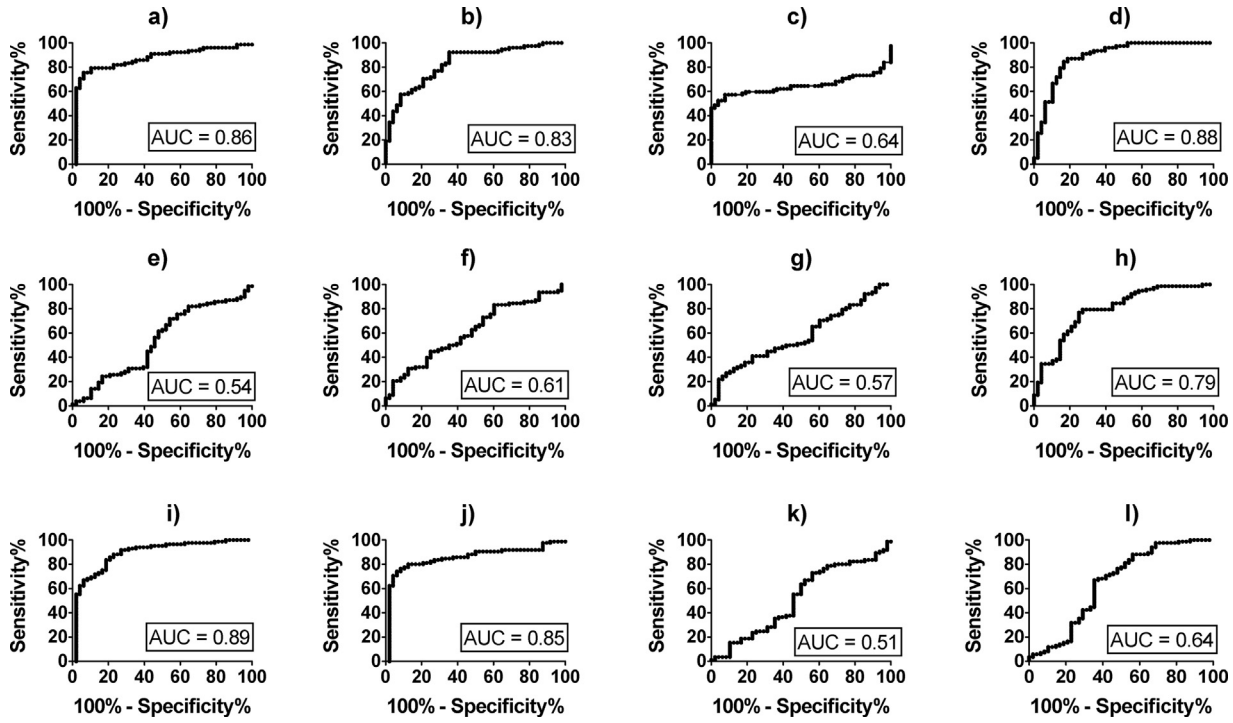

Fig. 4. ROC curves and area under the curve (AUC) values for each marker analyzed. (a) Angle of the depolarization vector in the FP (R_f^α), (b) modulus of the depolarization vector in the FP (R_f^m), (c) angle of the repolarization vector in the FP (T_f^α), (d) modulus of the repolarization vector in the FP (R_f^m), (e) angle of the depolarization vector in the PP (R_t^α), (f) modulus of the depolarization vector in the PP (R_t^α), (g) angle of the repolarization vector in the PP (T_t^α), (h) modulus of the repolarization vector in the PP (T_t^α), (i) angle of the cardiac vector in the FP (RT_f^α), (j) modulus of the cardiac vector in the FP (RT_f^α), (k) angle of the cardiac vector in the PP (RT_t^α), and (l) modulus of the cardiac vector in the PP (RT_t^α).

(LCx) in 18 patients and right coronary artery (RCA) in 40 patients. The mean ± SD values for the angles and moduli in the FP together with the number of patients N belonging to those groups are displayed in Table 1 and its counterpart for the PP, in Table 2. Notice that the only parameter able to discriminate all three ischemia localization was the angle of the T-wave in the FP, $p < 0.0001$.

4. Discussion

Even though angles presented normal values either for health or ischemia in the FP, the disease group showed values clearly biased to the left, in the limit of the normality range [33]. This explained the success of the FP depolarization and repolarization main orientations in differentiating both groups and vindicated the FP as a good spatial reference frame to standardize cardiac activity directions. The angular decrease with disease refers to depolarization or repolarization loops tending to lean down to the abscises, being this behavior consistent with the literature [34].

Even though the parameters accounting for the ventricular gradient (RT_f^α and RT_f^m) failed to produce any statistical significance, they did present good ROC curves with suitable AUC values (RT_f^α: AUC = 0.89, RT_f^m: AUC = 0.85).

Accompanying angular changes, depolarization voltages significantly decreased ($p < 0.0001$) in ischemia as well. This finding showed up as a simple and powerful marker of ischemia in humans (AUC = 0.83), expanding the results found in a model of myocardial infarction in rhesus monkeys, where the decrease of the R-wave amplitude turned out as a predictor of myocardial ischemia [35]. Consistently, Romero et al. also found evidence of angular changes in the QRS-complexes undergoing ischemia, suggesting a reduction in the depolarization voltages, measured on the same set of ischemic patients (from STAFF-III database) [9].

Table 1
Mean ± SD of frontal plane indexes for three different ischemia sites (STAFF-III database), [1] vs LCx, $p < 0.05$, [2] vs RCA, $p < 0.05$, [3] vs LCx, $p < 0.0001$, [4] vs RCA, $p < 0.0001$, [5] vs all, $p < 0.0001$.

	R_p^α (°)	R_p^m (mV)	T_p^α (°)	T_p^m (mV)	RT_p^α (°)	RT_p^m (mV)	N
LAD	29.38 ± 31.53[4]	0.13 ± 0.05[3]	56.04 ± 45.34[5]	0.82 ± 0.24[3]	34.53 ± 28.63	0.91 ± 0.26	25
LCx	27.82 ± 26.88	0.10 ± 0.03[4]	35.77 ± 60.18[5]	0.67 ± 0.15	29.03 ± 26.39	0.72 ± 0.18	18
RCA	24.87 ± 25.62	0.12 ± 0.06	−6.24 ± 57.68[5]	0.84 ± 0.30[4]	22.82 ± 24.78	0.91 ± 0.33	40

Table 2
Mean ± SD of preferential plane indexes for three different ischemia sites (STAFF-III database), [1] vs LCx, $p < 0.05$, [2] vs RCA, $p < 0.05$, [3] vs LCx, $p < 0.0001$, [4] vs RCA, $p < 0.0001$, [5] vs all, $p < 0.0001$.

	R_p^α (°)	R_p^m (mV)	T_p^α (°)	T_p^m (mV)	RT_p^α (°)	RT_p^m (mV)	N
LAD	0.59 ± 33.17[1]	0.97 ± 0.06[1]	−36.00 ± 80.94[4]	0.16 ± 0.09	−3.26 ± 32.35	1.05 ± 0.12	25
LCx	−17.13 ± 65.18	0.96 ± 0.07[2]	−21.31 ± 91.44[4]	0.16 ± 0.06[4]	−17.68 ± 69.00	1.01 ± 0.17	18
RCA	−13.24 ± 25.62	0.97 ± 0.06	−42.18 ± 107.18	0.21 ± 0.10	−21.31 ± 73.47	1.03 ± 0.16	40

The reduction in ECG voltage sounds sensible and consistent with the electrophysiological changes that ischemia induces at cellular level. First of all, ischemia moves metabolism from an aerobic to an anaerobic state, leading to a marked pH decrease. Also, ionic abnormal movements occur, moving into the cell big amounts of sodium, which takes the membrane potential to less negative levels, which in turn, forces more sodium channels to the inactivation state. The latter reduces the inward sodium current and thus, the amplitude and duration of the action potential [36]. After all these changes, a reduction in ECG voltages makes sense in physiological terms.

In a similar approach to ours, Ghista et al. presented a method to measure amplitude and direction of the electrical vector of the heart in a plane defined by Lead I and Lead II [37]. They derived the depolarization loops from these leads and measured two parameters on the loops: length and area. Length was equivalent to moduli in our work, and area together with another qualitative measure, quadrant occupation, helped separate different cardiac patterns such as normal sinus rhythm, left ventricular hypertrophy, bundle branch block (no particular separation regarding left or right) and myocardial infarction. Direction in angle as measured in our work, additionally to quadrant occupation and area of the loop could turn out as a complete descriptor of the loops, improving the separation of healthy and PTCA patients. Nevertheless, we believe that the analysis of loops derived from Lead I and Lead aVF makes more sense in a clinical environment, where there exist most of the evidence the medicine has based on.

With respect to the ventricular gradient, our results are comparable to those in Bortolan et al., where it was shown that the angles between QRS and T-wave loop axes did not change significantly between healthy versus patients with ischemia [38]. Nevertheless, the modified angle between QRS and T-wave loop parameter proposed in [39], which were computed on the zero point of the VCG loop, showed to be statistically different between healthy subjects group from those with ischemia, myocardial infarction and both. Consistently with the results of this work, Bortolan and colleagues have shown that the ratio of maximum to mean T vector magnitude, equivalent to our parameter called modulus of the T-wave maximum cardiac vector, presented significance differences among ischemic patients and healthy subjects [38].

On the other hand, it was not possible to define a clear separation between groups in the PP based on the spatial orientations of the main cardiac vectors. Moreover, the healthy group presented such a high variability that it was impossible to even think of a normality range in the PP. This may sound sensible if we remember that PCA technique imposes on ECG data individually optimized rotations, failing to provide a unique referencial frame for all the subjects. In an effort to reduce such dispersion in the PP, an alternative global transformation was proposed, applying PCA to a set of control subjects altogether, instead of transforming each subject individually. This way, PCA was carried out on a matrix containing 70% of the healthy subjects, onto which the remaining healthy subjects and ischemic patients were projected to generate the QRS-complex and T-wave loops in s_1 and s_2. Unfortunately, this new arrangement did not improve the dispersion observed in the PP. This finding may sound controversial with that found in [17], where the TCRT, based on the R–T angle in the PCA space, is a good cardiac risk predictor in survivors of acute myocardial infarction (AMI). However, due to the main objective of this work was to compare parameters obtained from 2D planes, we did not make an analogy between the computation of the parameter TCRT proposed in [17] and our indices computed for the PP. Moreover, there are several differences, between the dataset in [17] and this work. The experimental design in [17] was a cohort while ours was a cross-sectional study. Also, all the patients belonging to Zabel's study had suffered AMI while only a 30% of the STAFF-III database suffered a previous myocardial infarct. Therefore we have considered this as a limitation of the present study.

Opposite to angle measurements, amplitudes have significantly discriminated disease from health in the PP, specially the T-wave amplitude. This means that the PP is informative regarding signal energy information and plus, that signal energy lowers in silent ischemia, specially in the repolarization phase. This fact is important since the amplitudes in the FP only account for the energy contained in the frontal leads while the PP amplitudes contain the energy of the all eight independent leads. Thus, a decrease in amplitude in the PP reflects a net decrease in the ECG energy. Moreover, due to the transformation procedure, where the whole signal is first SVD-transformed and then segmented, and observing the greatest amplitude decrease in the T-wave, it can be proved that the greatest amount of energy decrease belongs to the repolarization phase.

It is important to notice that even though the representation of cardiac vectors in the SVD plane failed to produce angular parameters sensitive enough to discriminate silent ischemia, this does not apply for other parameters or indexes in this space. Moreover, much of the literature endorse this observation with plenty of examples, such as the complexity of repolarization C_r [40], the Total cosine R-to-T T_{crt} [16], the T-wave residuum T_{wr} [41] and the T-wave morphology dispersion T_{md} [42]. Even though all of the former parameters are defined in the 3D space except for the T_{md}, they all can be adapted to a 2D space. This will be addressed in Section 7.

Regarding ischemia localization, the repolarization main vector in the FP turned out to be the only parameter that allowed the simultaneous separation of the three groups LAD, LCx and RCA. This fact is good enough considering that most attempts to discriminate ischemia localization are carried out by means of body surface recordings, technique that takes several more electrodes than the ECG [43].

In this regard, Rubulis et al. [44] investigated the T-wave vector and loop characteristics in coronary artery disease (CAD) groups (LAD, LCx and RCA) and during PTCA. They have observed that the T-wave loop morphology (area and eigenvalues relationship) was significantly different in CAD patients and controls, while T-wave angles did not separate the groups. Conversely we noticed that the only parameter able to discriminate all three ischemia localization was the angle of the T-wave in the FP (see Table 1). It must be highlighted that, unlike in our present work, Rubulis et al. compared CAD groups during PTCA procedure.

5. Study limitations

A consideration regarding amplitude discrimination should be made, since data come from two different digital acquisition systems. Although both sets of data were weighed accordingly, differences in the analog–digital-converter (ADC) resolution could produce this kind of discrepancies. In that regard, there is a 0.1 μV difference in in the least significant bit (LSB) of both systems, being the one of the healthy group more accurate (LSB = 0.5 μV) than that of the PTCA patients (LSB = 0.6 μV). Nevertheless, we are confident that differences in ECG voltages are not affected by resolution differences, since amplitudes in the PTCA group resulted lower than the control group, opposing the tendency imposed by the excess error due to a broader resolution.

Finally, one limitation of this study is the marked difference between the mean age of the two populations (healthy subjects and ischemic patients). In order to search for an eventual correlation between the parameters involved in this study and age for both populations, the Pearson's correlation coefficient r between age and every parameter has been computed. The r-values have

been close to 0 and p-values have been greater than 0.05, thus, evidence supports that there is no significant correlation between the parameters measured over the depolarization/repolarization vectors and the patients age. Moreover, we have analyzed a subset of patients younger than 70 years old from the PTCA group and results kept very close to those presented here, accounting for the entire group. As a matter of fact, the age-corrected subset of PTCA patients produced more significant differences ($p < 0.0005$) for the parameters R_f^α, R_f^m, T_f^α, T_f^m, all of them belonging to the FP.

6. Conclusion

The FP offered a good fixed spatial reference frame that enabled a 2D representation sensitive to changes in the main depolarization and repolarization vectors due to silent ischemia. This effective separation between health and disease held for amplitudes and angles. The PP did not provide useful angular information due to its individual-optimized nature but did prove to pick up energy changes between groups. The latter also proved that ECG (mainly the repolarization phase) underwent a decrease in its energy during silent ischemia and led to the conclusion that information of the PP relies on the signal energy and not on axis orientation.

7. Future work

As future work, it can be mentioned the further study of the ability of classical PCA parameters of the literature, adapting them to the 2D space when corresponding and comparing them with the frontal plane. Furthermore, comparisons between the frontal plane and more complex spaces like the 3D space defined by the dipolar components *s1*, *s2* and *s3*, after SVD transformation of the ECG data should complete the insight into optimal ECG representations to better diagnose silent ischemia.

References

[1] E. Downar, M. Janse, D. Durrer, The effect of acute coronary artery occlusion on subepicardial transmembrane potentials in the intact porcine heart, Circulation 56 (1977) 217–223.

[2] M.J. Janse, A.L. Wit, Electrophysiological mechanisms of ventricular arrhythmias resulting from myocardial ischemia and infarction, Physiol. Rev. 69 (1989) 1049–1069.

[3] J. Pettersson, O. Pahlm, E. Carro, L. Edenbrandt, M. Ringborn, L. Sörnmo, S. Warren, G. Wagner, Changes in high-frequency QRS components are more sensitive than ST-segment deviation for detecting acute coronary artery occlusion, J. Am. Coll. Cardiol. 36 (6) (2000) 1827–1834.

[4] J. García, P. Lander, L. Sörnmo, S. Olmos, P. Wagner, G. Laguna, Comparative study of local and Karhunen–Loéve-Based ST-T indexes in recording from human subjects with induced myocardial ischemia, Comput. Biomed. Res. 31 (1998) 271–292.

[5] E. Pueyo, L. Sörnmo, P. Laguna, QRS slopes for detection and characterization of myocardial ischemia, IEEE Trans. Biomed. Eng. 55 (2) (2008) 468–477.

[6] N.B. Wagner, D.C. Sevilla, M.W. Krucoff, K.L. Lee, K.K. Pieper, R.K. Bottner, R.H. Selvester, G.S. Wagner, Transient alterations of the QRS complex and ST segment during percutaneous transluminal balloon angioplasty on the left anterior descending coronary artery, Am. J. Cardiol. 62 (1988) 1038–1042.

[7] S. Charlap, J. Shani, N. Schulho, B. Herman, E. Lichstein, R- and S-wave amplitude changes with acute anterior transmural myocardial ischaemia, Chest 97 (3) (1990) 566.

[8] P. Weston, L. Johanson, C. Schwartz, R. Maynard, R. Jennings, S. Wagner, The value of both ST-segment and QRS complex changes during acute coronary occlusion for prediction of reperfusion-induced myocardial salvage in a canine model, J. Electrocardiol. 40 (2007) 1825.

[9] D. Romero, M. Ringborn, P. Laguna, E. Pueyo, Detection and quantification of acute myocardial ischemia by morphologic evaluation of qrs changes by an angle-based method, J. Electrocardiol. 46 (2013) 204–214.

[10] R. Correa, P. Arini, M. Valentinuzzi, E. Laciar, Novel set of vectocardiographic parameters for the identification of ischemica patients, Med. Eng. Phys. 35 (2013) 16–22.

[11] G. Amit, O. Galante, L.R. Davrath, O. Luria, S. Abboud, D. Zahger, High-frequency QRS analysis in patients with acute myocardial infarction: a preliminary study, Ann. Noninvasive Electrocardiol. 18 (2) (2013) 149–156.

[12] N.J. Wimmer, B.M. Scirica, P.H. Stone, The clinical significance of continuous ECG (ambulatory ECG or holter) monitoring of the ST-segment to evaluate ischemia: a review, Progr. Cardiovasc. Dis. 56 (2) (2013) 195–202.

[13] F. Wilson, A.G. Mac Leod, P.S. Barker, F.D. Johnston, A. Arbor, The determination and the significance of the areas the ventricular deflections of the electrocardiogram, Am. Heart J. 10 (1934) 47–60.

[14] E. Cabrera, Teoría y Práctica de la Electrocardiografía, La prensa médica Mexicana, 1963.

[15] M. Vandyck-Acquah, P. Schweitzer, Ischaemic patterns: electrocardiographic background, in: Dynamic Electrocardiography, Blackwell Futura, 2004.

[16] B. Acar, G. Yi, K. Hnatkova, M. Malik, Spatial, temporal and wavefront direction characteristics of 12-lead T-wave morphology, Med. Biol. Eng. Comput. 37 (1999) 574–584.

[17] M. Zabel, B. Acar, T. Klingenheben, M.R. Franz, S.H. Hohnloser, M. Malik, Analysis of 12-lead T wave morphology for risk stratification after myocardial infarction, Circulation 102 (2000) 1252–1257.

[18] I. Kardys, J. Kors, I.e.a. van der Meer, Spatial QRS-T angle predicts cardiac death in a general population, Eur. Heart J. 24 (2003) 1357–1364.

[19] T. Yamazaki, V. Froelicher, J.e.a. Myers, Spatial QRS-T angle predicts cardiac death in a clinical population, Heart Rhythm 2 (2005) 73–78.

[20] R. Gajulapalli, A. Aneja, A. Rovner, Cardiac stress testing for the diagnosis and management of coronary artery disease: a reference for the primary care physician, South. Med. J. 105 (2) (2012) 93–99.

[21] W. Schuepbach, B. Emese, P. Loretan, A. Mallet, F. Duru, E. Sanz, B. Meier, Non-invasive diagnosis of coronary artery disease using cardiogoniometry performed at rest, Swiss Med. Wkly. 138 (15) (2008) 210–218.

[22] T. Huebner, W. Schuepbach, A. Seeck, E. Sanz, B. Meier, A. Voss, R. Pilgram, Cardiogoniometric parameters for detection of coronary artery disease at rest as a function of stenosis localization and distribution, Med. Biol. Eng. Comput. 48 (2010) 435–446.

[23] R. Bousseljot, D. Kreiseler, A. Schnabel, Nutzung der ekg-signaldatenbank cardiodat der PTB über das internet, Biomedizinische Technik 40 (1) (2001).

[24] A. Goldberger, L. Amaral, L. Glass, J. Hausdorff, P. Ivanov, R. Mark, J. Mietus, G. Moody, C. Peng, H. Stanley, Physiobank, physiotoolkit, and physionet: components of a new research resource for complex physiologic signals, Circulation 10 (23) (2000) e215–e220.

[25] M. Ringborn, J. Pettersson, E. Persson, S. Warren, P. Platonov, O. Pahlm, G. Wagner, Comparison of high-frequency qrs components and st-segment elevation to detect and quantify acute myocardial ischemia, J. Electrocardiol. (2010) 113–120.

[26] G.B. Moody, R.G. Mark, Development and evaluation of a 2 lead ECG analysis program, Comput. Cardiol. (1982) 39–44.

[27] J. Mendieta, Algoritmo para el delineado de senales electrocardiograficas en un modelo animal empleando tecnicas avanzadas de procesamiento de senales, Fac. de Ingenieria, Univ. de Buenos Aires (UBA), 2012 (Master's thesis).

[28] L. Sörnmo, Vectorcardiographic loop alignment and morphologic beat-to-beat variability, IEEE Trans. Biomed. Eng. 45 (12) (1998) 1401–1413.

[29] G. Breithardt, M. Cain, N. ElSherif, N. Flowers, V.J.M. Hombach, Standards for analysis of ventricular late potentials using high resolution or signal averaged electrocardiography: a statement by a task force committee of the European society of cardiology, the American heart association, and the European society of cardiology, and the American college of cardiology, Circulation 83 (1991) 1481–1488.

[30] K.S. Arun, T.S. Huang, Least-squares fitting of two 3-D point sets, IEEE Trans. Pattern Anal. Mach. Intell. 9 (5) (1987) 698–700.

[31] D. Altman, Practical Statistics for Medical Research, Chapman Hall, 26 Boundary Row, London, 1991.

[32] J.W. Hurst, Thoughts about the ventricular gradient and its current clinical use (part i of ii), Clin. Cardiol. 28 (2005) 175–180.

[33] J.W. Hurst, Thoughts about the ventricular gradient and its current clinical use (part ii of ii), Clin. Cardiol. 28 (2005) 219–224.

[34] J.A. Kors, G. van Herpen, J.H. van Bemmel, QT dispersion as an attribute of T-loop morphology, Circulation 99 (1999) 1458–1463.

[35] X. Sun, J. Cai, X. Fan, P. Han, Y. Xie, J. Chen, Y. Xiao, Y.J. Kang, Decreases in electrocardiographic r-wave amplitude and qt interval predict myocardial ischemic infarction in rhesus monkeys with left anterior descending artery ligation, PLoS ONE 8 (8) (2013) e71876.

[36] H. Engblom, D. Strauss, Multimodal Cardiovascular Imaging, McGraw Hill Medical, 2011.

[37] D. Ghista, U. Acharya, T. Nagenthiran, Frontal plane vectorcardiograms: theory and graphics visualization of cardiac health status, J. Med. Syst. 34 (4) (2010) 445–458.

[38] G. Bortolan, I. Cristov, Myocardial infarction and ischemia characterization from T-loop morphology in VCG, Comput. Cardiol. 28 (2001) 633–636.

[39] G. Bortolan, M. Bressan, I. Cristov, Review on the diagnostic potentials of the t-loop morphology in vcg, Bio Autom. 13 (2009) 55–71.

[40] S. Priori, D. Mortara, C. Napolitano, L. Diehl, V. Paganini, F. Cantú, G. Cantú, P. Schwartz, Evaluation of the spatial aspects of T wave complexity in the long-QT syndrome, Circulation 96 (1997) 3006–3012.

[41] M. Malik, B. Acar, Y. Gang, Y.G. Yap, K. Hnatkova, A.J. Camm, QT dispersion does not represent electrocardiographic interlead hetereogeneity of ventricular repolarization, J. Cardiovasc. Electrophysiol. 11 (2000) 835–843.
[42] M. Zabel, M. Malik, Practical use of T wave morphology assessment, Cardiac. Electrophys. Rev. 6 (3) (2002) 316–322.
[43] D. Mirvis, Differential electrocardiographic effects of myocardial ischemia induced by atrial pacing in dogs with various locations of coronary stenosis, Circulation 68 (5) (1983) 1116–1126.
[44] A. Rubulis, J. Jensen, G. Lundahl, J. Tapanainen, L. Wecke, L. Bergfeldt, T vector and loop characteristics in coronary artery disease and during acute ischemia, Heart Rhythm 3 (2004) 317–325.